

Multi-modal imaging reveals a small subpopulation of *Deinococcus radiodurans* exhibiting correlated metabolic activities

Weinan Zhu¹, Xinyu He¹, Haoran Li¹, Bo Jiang¹, Ruo-Chen Xie¹, and Wei Wang¹

¹Nanjing University

April 12, 2022

Abstract

Since a polyvalent strategy has recently been assumed to be adopted by *Deinococcus radiodurans* that can generate various resistance against many different detrimental sources of oxidative damage (e.g. reactive oxygen species, heavy metal ions and ionising radiation), investigating more than one restorative metabolic activities and their interrelation of the very same entities of *Deinococcus radiodurans* is of great significance for exploring its polyextremophile nature, which will be insightful for obtaining fundamental generic insights into life sustainability. Herein, we apply mainly fluorescence microscopy and back reflection microscopy to visibly assess the respective activities of superoxide radical generation and silver ion metabolism for individual *Deinococcus radiodurans*. Strikingly, only a minority (<20%) of the bacteria which show low superoxide radical levels is revealed to exhibit considerable formation of silver nanoparticles whilst those containing more superoxide radicals all show minimum silver ion metabolism. The discovery of the strong negative correlation for the small subpopulation between the two visualised different metabolic activities not only provides direct experimental evidence in terms of bacterial functionality for the inferred survival regime of the extreme microbe, but also suggests a new way of chemically examining biology from the perspective of inter-functional relationship.

Multi-modal imaging reveals a small subpopulation of *Deinococcus radiodurans* exhibiting correlated metabolic activities

Weinan Zhu¹, Xinyu He¹, Haoran Li¹, Bo Jiang¹, Ruo-Chen Xie¹, Wei Wang¹

¹State Key Laboratory of Analytical Chemistry for Life Science, School of Chemistry and Chemical Engineering, Chemistry and Biomedicine Innovation Center (ChemBIC), Nanjing University, Nanjing, China.

Correspondence

Ruo-Chen Xie and Wei Wang

Email: crxie@nju.edu.cn (R.C. Xie); wei.wang@nju.edu.cn (W. Wang)

Funding information

National Natural Science Foundation of China, Grant Numbers: 21925403 and 21874070;

Excellent Research Program of Nanjing University, Grant Numbers: ZYJH004.

Abstract

Since a polyvalent strategy has recently been assumed to be adopted by *Deinococcus radiodurans* that can generate various resistance against many different detrimental sources of oxidative damage (e.g. reactive oxygen species, heavy metal ions and ionising radiation), investigating more than one restorative metabolic activities and their interrelation of the very same entities of *Deinococcus radiodurans* is of great significance

for exploring its polyextremophile nature, which will be insightful for obtaining fundamental generic insights into life sustainability. Herein, we apply mainly fluorescence microscopy and back reflection microscopy to visibly assess the respective activities of superoxide radical generation and silver ion metabolism for individual *Deinococcus radiodurans*. Strikingly, only a minority (<20%) of the bacteria which show low superoxide radical levels is revealed to exhibit considerable formation of silver nanoparticles whilst those containing more superoxide radicals all show minimum silver ion metabolism. The discovery of the strong negative correlation for the small subpopulation between the two visualised different metabolic activities not only provides direct experimental evidence in terms of bacterial functionality for the inferred survival regime of the extreme microbe, but also suggests a new way of chemically examining biology from the perspective of inter-functional relationship.

Key points

- The use of back reflection microscopy allows the discovery of a small subpopulation of *Deinococcus radiodurans* exhibiting extraordinary silver ion metabolism.
- Combining fluorescence microscopy and bright field microscopy we further show the subpopulation all contain correlated relatively low levels of superoxide radicals.
- The findings from the angle of exploring inter-functional relationship directly supports the polyvalent strategy currently proposed for the polyextremophile for survivals against various sources of oxidative damage.

KEYWORDS

optical microscopy, subpopulation, extremophile, *Deinococcus radiodurans*, oxidative damage, heavy metal metabolism, reactive oxygen species.

1. Introduction

The survival of the polyextremophile *Deinococcus radiodurans* (*D.r.*) under a variety of extreme conditions raises the question of the underlying mechanism. Unravelling the mechanism of this particular microbe is expected to greatly improve the understanding of the principles of life sustainability in general. The current mainstream view is that the fact is likely based on a single polyvalent, rather than multiple parallel (each for a specific condition), strategy generating various resistances.¹ The key of the strategy lies in the presence of a strong proteome protection system that consists of an antioxidant fraction of the *D.r.* cytosol with a small molecular weight of less than 3 kDa,^{2, 3} and otherwise protein carbonylation can easily occur and cause cell death *via* irreversible and progressive degeneration of most vital cellular functions.^{4, 5} Such a constitutive protection is thus considered to possibly cope with many different sources causing oxidative damages including reactive oxygen species,² heavy metal ions⁶⁻⁹ and ionising radiation¹⁰⁻¹². While the identity of the antioxidant system is largely revealed, direct experimental evidence of the bacterial multifunction and inter-function relationship is needed to testify or consolidate the inferred regime for the unusual resilience of the creature.

The functionality of a bacterium is, however, of a complex origin. Even within a bacterial culture of a same genome, phenotypic heterogeneity would occur and contribute the functional diversity to microbial populations.^{13, 14} Statistical fluctuation, for example, leads to a random generation of subpopulations with distinct gene expressions.¹⁵⁻¹⁷ Alternatively, heterogeneity can possibly be driven by environmental changes¹⁸ and results in a small subpopulation with phenotypic differences from the rest of the culture.¹⁹⁻²¹ Quorum sensing of pathogenic bacteria can yield such type of heterogeneity to protect themselves against host attack.^{22, 23} These discoveries imply that the major body of current research on the biochemical properties of bacteria, which is mainly based on the bulk analysis (e.g. ion chromatography,⁶ UV/vis and infrared spectroscopy^{7, 8, 24}) of the extracts of intra- or extracellular contents, can hardly resolve the function profile of a particular bacterium on a colony basis. Therefore, studying more than one biological activities and their interrelation at the single bacterium level is crucial to provide unambiguous fundamental insights into the complex behaviour of a bacterial strain.

Given the desired spatial resolutions and the non-invasive nature of optical microscopic techniques for studying single living cells under various conditions,²⁵⁻²⁹ in this work we apply optical microscopy under suitable imaging modes for different species as a major means to visibly characterise two different biological activities of superoxide radical (SR) generation and silver ion metabolism of individual bacteria. Although metal ion metabolism can increase the production of reactive oxygen species,³⁰ the metabolic pathways of the silver ion reduction and superoxide radical generation have not shown any relation in the literature. We discover that these two seemingly independent capacities of the bacteria are clearly correlated and this occurs only within a small subgroup (<20%) of a clonal population. Note that we clarify here as the *D.r.* bacteria predominantly appear as four linked bodies while the latter is distinctly separate from all others, the term ‘individual bacteria’ used in this work actually means the entity of the tetracocci form.

2. Experimental

2.1. Chemicals and bacterial cultures

AgNO₃, HCl, NaOH, and sodium alginate were purchased from Sigma Aldrich, USA, dihydroethidium (DHE) from Yeasen Biotechnology, China and both PBS buffer solution (135 mM NaCl, 4.7 mM KCl, 10 mM Na₂HPO₄, 2 mM NaH₂PO₄, pH=7.3±0.1) and polydimethylsiloxane (PDMS) were from Beyotime Biotechnology, China. All these reagents were analytical-grade and used as received. All solutions were prepared with Milli-Q ultrapure water (18 MΩ-cm, Thermo Fisher).

Deinococcus radiodurans Strain R1 (ATCC 13939) was grown from a single bacterium aerobically (under atmospheric conditions) at 30°C in peptone yeast glucose (PYG) broth (containing 2% peptone, 0.5% glucose, 1% yeast extract, pH 7.2) with agitation at 300 rpm. The pH of the broth was adjusted to 7 by adding hydrochloric acid or sodium hydroxide. The bacterial growth was assessed by measuring optical density (OD) *via* a microplate reader (see below Section 2.2.3) at the wavelength of 600 nm of the strain. The OD value stayed stable since reaching 1.0, and the *D.r.* strain at this stage was considered to have a stable population and morphology, and therefore selected to be used throughout the experiment. For obtaining the bacteria containing silver particles, the grown culture above was cultivated in a fresh PYG broth initially containing 2.0 mM AgNO₃ with a pH of 7 and at 30 for another 9 hours. The bacteria after incubation in AgNO₃ solutions were centrifuged at 8000xg to collect the microbes and washed with PBS for further analysis.

2.2. Apparatus and measurements

2.2.1. Optical set-up and the microscopic measurements

The microscopic imaging and measurements were performed on a commercial inverted microscope (Nikon, Ti-E), which was equipped with a 60X objective lens with a numerical aperture (NA) of 1.49. Depending on the studied species, the microscope was operated under three different modes: fluorescent, bright field, back-reflection. In the fluorescence mode, a white-light diode (X-cite^(r) 110LED, Excelitas Technologies) coupled with a bandpass filter (450–490 nm) was used to excite DHE-induced fluorophores. A digital CMOS camera (C11440, Hamamastu) was used to collect the fluorescence signals, and a long-pass filter ($\lambda > 520$ nm) to prevent the excitation light from entering the camera. The back-reflection mode using the same light path as that of the fluorescent mode was achieved by using a 520-560 nm bandpass filter for the illumination light (to avoid fluorescent excitation when the solution contained DHE molecules), and also removing the long-pass filter. As such, only the back reflected green light signals were collected. The two imaging modes were switched by converting the filter cube manually. In the bright field mode, the light source was a quartz tungsten halogen lamp (LV-LH50PC, Nikon) and used without any optical filters. The three modes shared the same camera as above.

For fluorescence analysis, the bacteria containing Ag particles were prepared as a bacterial solution with a concentration of 2×10^8 mL⁻¹ using PBS buffer, and DHE was added into the latter with a final concentration of 100 μ M. The mixture was incubated at 30 for 1 hour and then washed using PBS buffer to remove the excess DHE molecules. A 100 μ L of the washed mixture was added into a PDMS chamber with a sodium

alginate-modified glass substrate and let it stand still for 10 minutes. Consequently, the bacterial cells were observed to adsorb strongly onto the glass wall forming a monolayer. PBS was used to gently rinse the mixture in the chamber for the removal of suspended bacteria. As such, the adhered bacteria were studied using the fluorescence microscopy described above. The sample preparation for the bright field and back reflection imaging was all the same but the DHE molecules were not added in the experiments described in Section 3.2.

2.2.2. Flow cytometry

Scattering properties of silver-containing bacteria were measured using a CytoFlex S flow cytometer (Beckman Coulter). The bacterial mixture was transferred to the sheath fluid with a bacterial concentration of 10^5 mL⁻¹ for flow cytometry. Next, with the laser beam passing the bacteria in the fluid, both forward scattering and side scattering signals of those bacteria were detected and analysed. In addition, specific concentrations of bacteria in a solution were measured by flow cytometry.

2.2.3. Microplate reader

The monitoring of OD values and the UV-vis spectra of the bacterial mixtures used in this work were conducted using a multifunctional microplate reader (SynergyLX, Biotek/Agilen). The OD measurements were done on the original mixture of the bacteria with the broth, whilst the UV-vis spectra were measured for the silver-containing bacteria that were re-suspended in PBS buffer solutions.

2.2.4. Electrochemical measurements

The electrochemical measurements was performed using a CS120 electrochemical work station (CorrTest, China). A three-electrode system was used for the measurement, where a gold disc electrode (d=3.0 mm, Tianjin Aida, China; the same brand for other electrodes below) was used as the working electrode, an Ag/AgCl (saturated KCl, $E^\circ = 0.190$ V vs. standard hydrogen electrode) was used as the reference electrode and a platinum sheet as the counter electrode. The electrodes were inserted into a solution of *D.r.* bacteria (with a concentration of 2×10^8 mL⁻¹) which was directly taken from the incubation mixture with the PYG broth. Next, anodic stripping voltammetry was applied every 1.5 hours to monitor the silver ion concentration of the bulk solution within a total period of 9 hours. Specifically, the stripping voltammetry was conducted by applying in sequence a surface-refreshing potential of 0.6 V vs. Ag/AgCl for 60 seconds, a pre-concentration potential of -0.45 V for 60 seconds again, and a potential cycle between 0.0 and 0.6 V at a scan rate of 0.1 V s⁻¹.

2.2.5. Scanning electron microscopy

Electron microscopic imaging was performed using a JEOL JSM-7800F Scanning Electron Microscope (SEM) equipped with Energy Dispersive Spectroscopy (EDS). The silver particle-containing bacteria were dropcast on to a cover glass and let dry overnight at room temperature, and after gold sputtering the immobilised bacteria were imaged using the electron microscope at an acceleration voltage of 15.0 kV. In addition, EDS was conducted on the selected areas of the sputtered glass for elemental analysis.

3. Results and discussion

3.1. Fluorescence analysis of the superoxide radical level in individual bacteria

The SR levels of individual bacteria were analysed using fluorescence microscopy. Experimentally, the mature bacteria (OD=1.0) were first resuspended in PBS buffer solutions and imaged using bright field microscopy. Figure 1a shows a total number of nearly 200 separate entities of bacteria in the view. Next, dihydroethidium (DHE) was added into the bacterial solution for use as a specific fluorescence probe to uncover the SR levels with a positive response. The DHE-uptaken bacteria were then immobilised on to a sodium alginate-modified coverglass and imaged using fluorescence microscopy at an excitation light wavelength of 510 nm. Consequently, Figure 1b presents all the *ca.* 200 bacteria observed in Figure 1a which now appear red, suggesting the superoxide radical generation is active all over the bacterial colony. The inset with a much better contrast than that in Figure 1a further resolves the structure of each entity of the bacteria and shows

their predominant existence as tetracocci. Importantly, it is seen that within the bacterial culture, their fluorescence (FL) intensities differ from each other. The FL intensity distribution as shown in the Figure 1c was obtained by measuring the integral intensity of the 2D area of each bacteria. It is therefore clear that individual bacteria exhibit different SR levels inside them, indicating the differences of their antioxidant capacities within the colony.

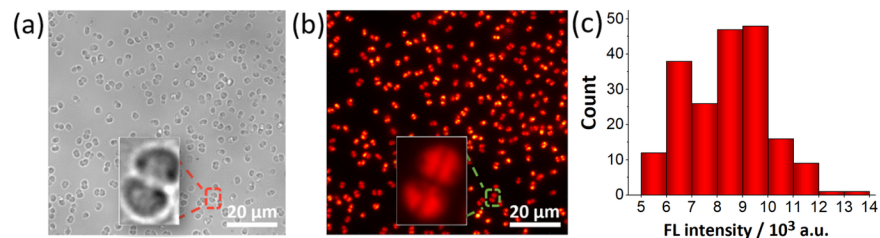


Figure 1. (a) Bright field and (b) fluorescence images of individual bacteria, while the insets enlarge a same single entity of a *D.r.tetracocci*. (c) FL intensity distribution.

3.2. Assessment of silver ion metabolism of individual *D.r.* bacteria

While the dissimilar SR levels of individual *D.r.* are clear, their abilities to reduce silver ions and to form less toxic Ag metal particles are carefully characterised both at the bulk level and the single bacterium level. First, anodic stripping voltammetry was conducted as a function of time to a gold macrodisc electrode inserted in a grown bacterial solution initially containing 2 mM silver ions and the broth compositions. Figure 2a shows throughout the experiment an oxidation peak at the potentials of 0.2~0.3 V in contrast to the blank voltammogram obtained with the bacterial solution without Ag⁺ added. This indicates that the peak corresponds to the oxidation of the reduced silver from the bacterial solutions in the pre-concentration step. Importantly, the charge transferred during the voltammetric peak was observed to gradually decrease to nearly none (<5%), suggesting an almost complete consumption of silver ions by the bacteria in the bulk solution over the 9 hours. This inference is on the basis that since the stripping of a monolayer deposition of silver is estimated to correspond to an oxidative charge of 14 μC (see Supporting Information Section 1 for the calculation), which is far more than the largest amount (~ 3 μC) measured in our experiment, the electrode used is thus thought to be large enough to minimise inhomogeneous surface redox reactions,³¹ and the measured charge can be quantitatively related to the silver ion concentration. Besides, it is noted that the negative shift of the peak potential over time, despite the inferred decrease in the silver ion concentration, is probably due to an increased level of halide anions in the extracellular solution that results from the microbial metabolism. Next, the resulting bacterial mixture with the minimum Ag⁺ content was briefly examined by UV-vis spectroscopy. In comparison with the bacteria incubated without silver ions, a distinct absorption band at around 430 nm was seen in Figure 2b, which coincides with the well-known characteristic wavelength of the plasmonic absorption of silver nanoparticles, suggesting the product of the silver ion uptake by the bacteria is metallic nanosilver.

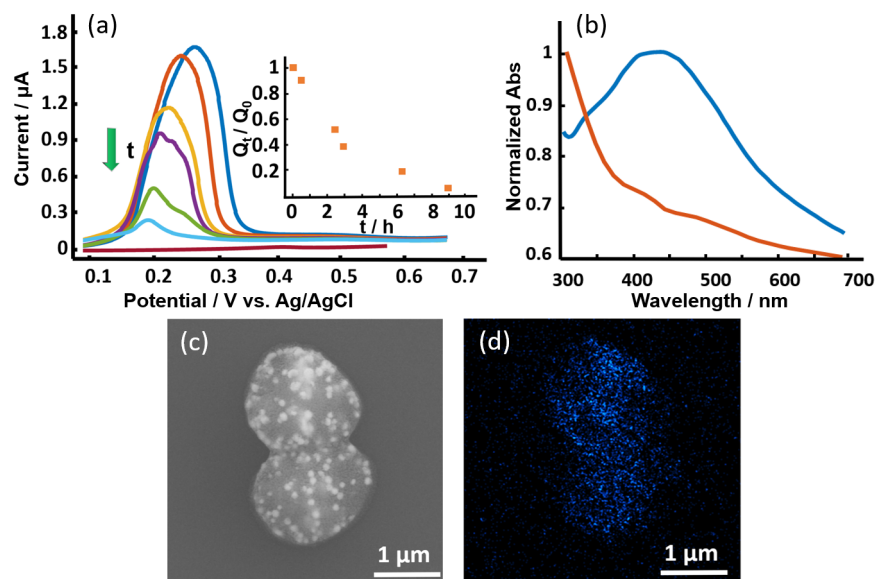


Figure 2. Consumption of Ag^+ ions and Ag nanoparticle formation of *D.r.* bacteria. (a) Anodic stripping voltammograms of bacterial solutions initially containing 2 mM AgNO_3 as a function of time within 9 hours. (b) UV-vis spectra of the bacteria with (red) and without (blue) Ag^+ incubation. (c) SEM image and (d) Ag-element mapping.

The product of the bacterial silver consumption is further investigated by looking into a single bacterium using scanning electron microscopy. Figure 2c shows a representative SEM image of a silver particle-containing bacterium. A total number of 106 bright features with an average diameter of 95 ± 22 nm within the bacterial cell is evident (see Figure S1). Furthermore, elemental mapping based on EDS (Figure 2d) shows the presence of silver and importantly the spatial distribution of the Ag element is well consistent with that in the electron microscopic image. These observations strongly confirm that inside the bacteria silver nanoparticles form as a result of the silver ion uptake. As such, the characterisations above clearly demonstrate the ability of individual *D.r.* bacteria to reduce the silver metal ions.

On the basis of the strongly scattering properties of silver nanoparticles, we next turn to optically explore the differences in the silver ion reducing ability of bacteria within their cultures. To this end, the high-throughput method of flow cytometry was conducted for detecting the bacteria after the incubation with Ag^+ and both the forward scattering and side scattering signals were collected for individual bacteria. It is recognised that forward scatter detection is mainly related to the size of a cell and thus for a certain bacterial strain a larger cell gives higher scattering intensity, whilst side scatter detection is relatively sensitive to the strongly scattering particles inside the cell.^{32, 33} The two kinds of scatter signals are plotted for each detected bacteria in form of a two dimensional intensity distribution graph as shown in Figure 3a& 3b. As a result, the scattering signals of bacteria after incubation with Ag^+ exhibit a bimodal distribution (Figure 3b) where the first contour peak at the SSC intensity of *ca.* 10^5 becomes larger than that for the bacteria before Ag^+ incubation (i.e. some 10^4) as shown in Figure 3a, which is consistent with the formation of the strongly scattering silver nanoparticles for most bacteria. Strikingly, a second, though smaller, peak emerges at a much higher SSC intensity of nearly 10^6 , indicating a unusually considerable number of silver nanoparticles formed in those bacteria. In contrast, the FSC intensity of the bacteria before and after Ag^+ incubation stays almost constant. Nevertheless, the bacteria synthesising large quantities of silver nanoparticles show a relatively higher FSC intensity than most bacteria on average, to which the scattering silver particles possibly contribute. Figure 3c shows the number distributions of bacteria with different SSC intensity before and after the Ag^+ incubation. While the total number of bacteria seems unchanged despite being incubated,

the after-incubation bacteria with the SSC values within the second peak account for a small portion of nearly 10% by integral. These observations implies the emergence of a minority of ‘strongly reducing’ bacteria that are distinct from the others in silver metal metabolism when exposed to silver ions. The phenomenon points to the interesting fact that when facing environmental threats, bacteria owning the same genome can evolve to a subpopulation of a very different phenotype – in this case, those that can reduce silver ions much more greatly than the rest. This natural strategy is consistent with the extraordinary adapting ability of the polyextremophile.

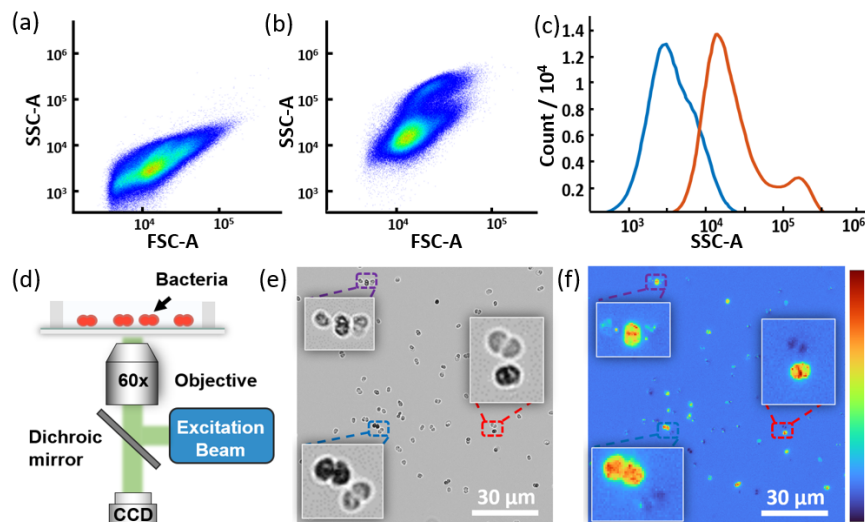


Figure 3. Flow cytometric detection of the bacterial populations in terms of side scattering and forward scattering without (a) and with (b) Ag^+ incubation. (c) Side scattering intensity distribution of the bacteria with and without Ag^+ incubation. (d) Schematics of back-illumination microscopy. (e) Bright-field image and (f) back-illumination image of bacteria in a same region of interest.

We further seek to distinguish the individual ‘strongly reducing’ bacteria visibly. Bright field microscopy is first applied to the bacteria mixture after Ag^+ incubation and washing with PBS buffers. Figure 3e shows that in the view over 100 bacteria is seen which yet exhibit very different contrasts. While most bacteria appear to be greyer than the background, a small portion shows somewhat even darker which is not observed in the control group (see Figure S2). Although bright field microscopy allows the observations of all the bacteria in the optical field, the difference in the contrasts between different bacteria is sometimes not very distinct (e.g. the upper left inset in Figure 3e). To improve the situation, we have developed an alternative imaging mode utilising the back reflection of a light beam that is able to presumably better distinguish between different types of bacterial cells. As shown in Figure 3d, the technique basically uses the same light path as that in fluorescent microscopy where a light beam illuminates the bacteria and reflect back to the camera, but in this back-reflection mode the light is not restricted to the narrow range of wavelength for fluorophore excitation. Consequently, Figure 3f insets show a more significant contrast between these bacteria – much greater optical intensity for the darker bacteria seen using the bright field mode (Figure 3e insets), while far lower intensity for the rest population. Moreover, the former type of bacteria is observed to be apparently fewer than the latter in the back reflection imaging mode, which is consistent with the results of the flow cytometric measurements. We thus assume the imaging mode is more sensitive to the internal silver nanoparticles. This imaging mode is therefore considered to be a well-suited approach to discern the bacteria of a strong capacity of silver metal metabolism from those of an average ability.

3.3. Correlated superoxide radical levels and silver nanoparticle levels of individual bacteria

Having evidenced the differing SR levels of bacteria using fluorescence microscopy and varying silver nanopar-

to determine the concentration of silver ions inside a bacterium using back reflection imaging, we finally investigate the possible correlation between the levels of two biologically redox active products at the single bacterium level. Experimentally, the DHE fluorescence probes were added to a bacterial mixture after the incubation with Ag^+ to create DHE-labelled Ag particle-containing bacteria. In turn, bright field microscopy, back reflection imaging and fluorescence microscopy were applied to the immobilised bacteria in a same optical field. Consequently, the optical intensity of respective images are compared for each single entity.

Surprisingly, as the bright field image in Figure 4a presents all the adhered bacteria in the optical field, a small fraction (<20%) of the bacteria exhibiting an exceptional back reflection intensity (Figure 4b) are shown to be exactly complementary to those exhibiting a high fluorescent intensity (Figure 4c). Ultimately, the fluorescent intensity and the back reflection intensity of a total number of 1626 bacteria were individually measured and plotted in the correlation chart (Figure 4d). Overall, a distinct negative correlation between the two kinds of optical signals is evident. This strongly suggests that a bacterium which has a potent ability to reduce silver ions tends to possess a low superoxide radical level. This conclusion further implies that the two different kinds of biological activities – superoxide radical reduction and silver ion reduction – may share to some extent the same reducing system within *D.r.* bacteria: in this case, the pool of antioxidant molecules in the bacterial cytosol as discussed in Introduction. On the ground that most single entity research focuses on structure-activity relationship, our work suggests an interesting perspective of looking into the relationship between different activities of a same microbe, which may gain fundamental implications for chemical aspects of biology.

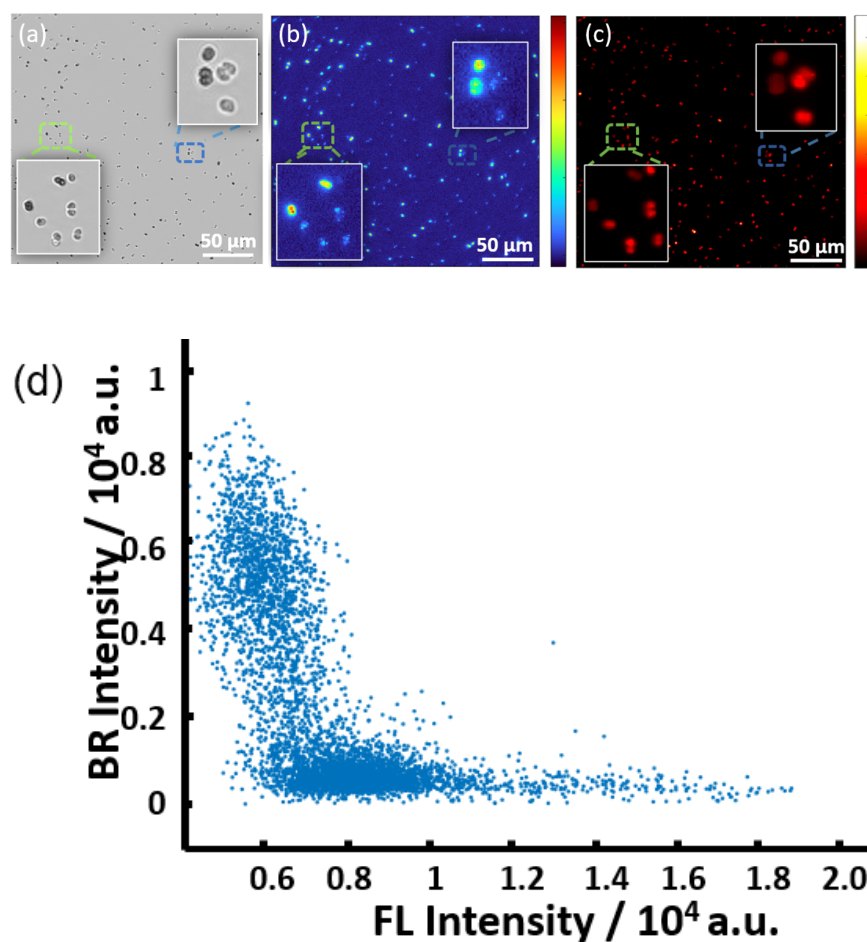


Figure 4. (a) A bright field, (b) back reflection and (c) fluorescent image of a same optical field of the DHE-labelled Ag particle-containing bacteria immobilised on a glass substrate in PBS buffer solutions. (d) Correlation chart between the back reflection (BR) intensity and fluorescence (FL) intensity of a considerable number of individual bacteria.

4. Conclusions

This work applies optical microscopy under varying imaging modes depending on the analyte species to visualise both metabolic activities of silver ion reduction and superoxide radical generation of the *D.r.* colony. It is discovered that a distinct negative correlation between the two biochemical processes surfaces yet only for a minor subpopulation of the bacteria. Interestingly, this finding directly supports the current view of the single polyvalent strategy against various conditions lethal to most species for explaining the polyextremophile nature of *D.r.* bacteria.

Acknowledgements

This research is funded by National Natural Science Foundation of China (Grant No. 21925403 and 21874070) and Excellent Research Program of Nanjing University (Grant No. ZYJH004).

Competing interest

The authors declare no competing financial interest.

References

1. Krisko, A.; Radman, M., Biology of extreme radiation resistance: the way of *Deinococcus radiodurans*. *Cold Spring Harbor perspectives in biology* **2013**, *5* (7), a012765.
2. Krisko, A.; Radman, M., Protein damage and death by radiation in *Escherichia coli* and *Deinococcus radiodurans*. *Proceedings of the National Academy of Sciences* **2010**, *107* (32), 14373-14377.
3. Daly, M. J.; Gaidamakova, E. K.; Matrosova, V. Y.; Kiang, J. G.; Fukumoto, R.; Lee, D.-Y.; Wehr, N. B.; Viteri, G. A.; Berlett, B. S.; Levine, R. L., Small-molecule antioxidant proteome-shields in *Deinococcus radiodurans*. *PloS one* **2010**, *5* (9), e12570.
4. Krisko, A.; Radman, M., Phenotypic and genetic consequences of protein damage. *PLoS genetics* **2013**, *9* (9), e1003810.
5. Po, K. H. L.; Chow, H. Y.; Cheng, Q.; Chan, B. K. w.; Deng, X.; Wang, S.; Chan, E. W. C.; Kong, H. K.; Chan, K. F.; Li, X., Daptomycin exerts bactericidal effect through induction of excessive ROS production and blocking the function of stress response protein Usp2. *Natural Sciences* **2021**, *1* (2), e10023.
6. Fredrickson, J. K.; Kostandarithes, H. M.; Li, S.; Plymale, A. E.; Daly, M., Reduction of Fe(III), Cr(VI), U(VI), and Tc(VII) by *Deinococcus radiodurans* R1. *Applied and Environmental Microbiology* **2000**, *66* (5), 2006-2011.
7. Kulkarni, R. R.; Shaiwale, N. S.; Deobagkar, D. N.; Deobagkar, D. D., Synthesis and extracellular accumulation of silver nanoparticles by employing radiation-resistant *Deinococcus radiodurans*, their characterization, and determination of bioactivity. *International journal of nanomedicine* **2015**, *10*, 963.
8. Li, J.; Webster, T. J.; Tian, B., Functionalized nanomaterial assembling and biosynthesis using the extremophile *Deinococcus radiodurans* for multifunctional applications. *Small* **2019**, *15* (20), 1900600.
9. Ge, C.; Huang, D.; Wang, D.; Zhang, E.; Li, M.; Zhu, F.; Zhu, C.; Chen, N.; Wu, S.; Zhou, D., Biotic Process Dominated the Uptake and Transformation of Ag⁺ by *Shewanella oneidensis* MR-1. *Environmental Science & Technology* **2022**, *56* (4), 2366-2377.
10. Daly, M. J.; Gaidamakova, E. K.; Matrosova, V. Y.; Vasilenko, A.; Zhai, M.; Leapman, R. D.; Lai, B.; Ravel, B.; Li, S.-M. W.; Kemner, K. M., Protein oxidation implicated as the primary determinant of bacterial radioresistance. *PLoS biology* **2007**, *5* (4), e92.

11. Daly, M. J., A new perspective on radiation resistance based on *Deinococcus radiodurans*. *Nature Reviews Microbiology* **2009**, *7* (3), 237-245.
12. Brim, H.; McFarlan, S. C.; Fredrickson, J. K.; Minton, K. W.; Zhai, M.; Wackett, L. P.; Daly, M. J., Engineering *Deinococcus radiodurans* for metal remediation in radioactive mixed waste environments. *Nature Biotechnology* **2000**, *18* (1), 85-90.
13. Davis, K. M.; Isberg, R. R., Defining heterogeneity within bacterial populations via single cell approaches. *Bioessays* **2016**, *38* (8), 782-790.
14. Ackermann, M., A functional perspective on phenotypic heterogeneity in microorganisms. *Nature Reviews Microbiology* **2015**, *13* (8), 497-508.
15. Ackermann, M.; Stecher, B.; Freed, N. E.; Songhet, P.; Hardt, W.-D.; Doebeli, M., Self-destructive cooperation mediated by phenotypic noise. *Nature* **2008**, *454* (7207), 987-990.
16. Sandoz, K. M.; Mitzimberg, S. M.; Schuster, M., Social cheating in *Pseudomonas aeruginosa* quorum sensing. *Proceedings of the National Academy of Sciences* **2007**, *104* (40), 15876-15881.
17. Dandekar, A. A.; Chugani, S.; Greenberg, E. P., Bacterial quorum sensing and metabolic incentives to cooperate. *Science* **2012**, *338* (6104), 264-266.
18. Rangarajan, A. A.; Koropatkin, N. M.; Biteen, J. S., Nutrient-dependent morphological variability of *Bacteroides thetaiotaomicron*. *Microbiology* **2020**, *166* (7), 624-628.
19. Helaine, S.; Thompson, J. A.; Watson, K. G.; Liu, M.; Boyle, C.; Holden, D. W., Dynamics of intracellular bacterial replication at the single cell level. *Proceedings of the National Academy of Sciences* **2010**, *107* (8), 3746-3751.
20. Eldar, A.; Elowitz, M. B., Functional roles for noise in genetic circuits. *Nature* **2010**, *467* (7312), 167-173.
21. Avery, S. V., Microbial cell individuality and the underlying sources of heterogeneity. *Nature Reviews Microbiology* **2006**, *4* (8), 577-587.
22. Davis, K. M.; Mohammadi, S.; Isberg, R. R., Community behavior and spatial regulation within a bacterial microcolony in deep tissue sites serves to protect against host attack. *Cell host & microbe* **2015**, *17* (1), 21-31.
23. Sánchez-Romero, M. A.; Casadesús, J., Contribution of phenotypic heterogeneity to adaptive antibiotic resistance. *Proceedings of the National Academy of Sciences* **2014**, *111* (1), 355-360.
24. Tian, B.; Li, J.; Pang, R.; Dai, S.; Li, T.; Weng, Y.; Jin, Y.; Hua, Y., Gold nanoparticles biosynthesized and functionalized using a hydroxylated tetraterpenoid trigger gene expression changes and apoptosis in cancer cells. *ACS applied materials & interfaces* **2018**, *10* (43), 37353-37363.
25. Chia, H. E.; Marsh, E. N. G.; Biteen, J. S., Extending fluorescence microscopy into anaerobic environments. *Current Opinion in Chemical Biology* **2019**, *51* , 98-104.
26. Chia, H. E.; Zuo, T.; Koropatkin, N. M.; Marsh, E. N. G.; Biteen, J. S., Imaging living obligate anaerobic bacteria with bilin-binding fluorescent proteins. *Current research in microbial sciences* **2020**, *1* , 1-6.
27. Xiong, B.; Zhou, R.; Hao, J.; Jia, Y.; He, Y.; Yeung, E. S., Highly sensitive sulphide mapping in live cells by kinetic spectral analysis of single Au-Ag core-shell nanoparticles. *Nature communications* **2013**, *4* (1), 1-9.
28. Xiong, B.; Huang, Z.; Zou, H.; Qiao, C.; He, Y.; Yeung, E. S., Single plasmonic nanosprings for visualizing reactive-oxygen-species-activated localized mechanical force transduction in live cells. *ACS nano* **2017**, *11* (1), 541-548.

29. Nikel, P. I.; Silva-Rocha, R.; Benedetti, I.; de Lorenzo, V., The private life of environmental bacteria: pollutant biodegradation at the single cell level. *Environmental Microbiology* **2014**, *16* (3), 628-642.
30. Ojuederie, O. B.; Babalola, O. O., Microbial and plant-assisted bioremediation of heavy metal polluted environments: a review. *International journal of environmental research and public health* **2017**, *14* (12), 1504.
31. Hyde, M. E.; Banks, C. E.; Compton, R. G., Anodic stripping voltammetry: an AFM study of some problems and limitations. *Electroanalysis* **2004**, *16* (5), 345-354.
32. Van Der Vlist, E. J.; Stoorvogel, W.; Arkesteijn, G. J.; Wauben, M. H., Fluorescent labeling of nano-sized vesicles released by cells and subsequent quantitative and qualitative analysis by high-resolution flow cytometry. *Nature protocols* **2012**, *7* (7), 1311-1326.
33. Robinson, J. P., Flow cytometry. *Encyclopedia of biomaterials and biomedical engineering* **2004**, *3* , 630-642.